THE JOURNAL OF PHYSICAL CHEMISTRY A

ARTICLE

pubs.acs.org/JPCA

Pulsed Jet Discharge Matrix Isolation and Computational Study of Bromine Atom Complexes: Br···BrXCH$_2$ (X = H, Cl, Br)

Lisa George,[†] Aimable Kalume,[†] Brian Esselman,[‡] Robert J. McMahon,[‡] and Scott A. Reid*[,†]

[†]Department of Chemistry, Marquette University, Milwaukee, Wisconsin 53233, United States

[‡]Department of Chemistry, University of Wisconsin—Madison, Madison, Wisconsin 53706, United States

Supporting Information

ABSTRACT: Halogen atoms are important reactive radicals in the atmosphere. In this work, pulsed jet discharge matrix isolation spectroscopy and computational methods were used to characterize prereactive complexes of halogen atoms with simple halons. Our experiments combined matrix isolation techniques with a pulsed DC discharge nozzle, where a dilute CH_2XBr (X = H, Cl, Br)/rare gas sample was gently discharged and the products were deposited onto a cold KBr window. The Br···$BrCH_2X$ (X = H, Cl, Br) complexes were characterized by infrared and electronic spectroscopy, supported by ab initio and density functional theory (DFT) calculations, which shed light on the structure of, bonding in, and binding energy of the complexes. The correlation of charge-transfer energy with donor ionization potential (Mulliken correlation) was examined, and the charge-transfer photochemistry of the complexes was explored.

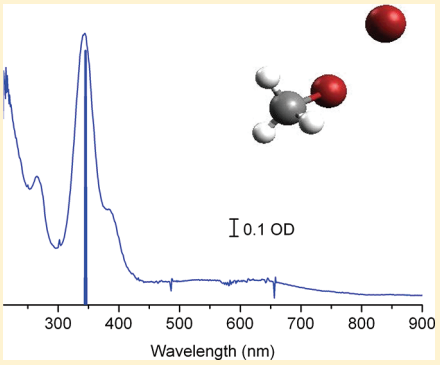

1. INTRODUCTION

Halogen atoms are well-known reactive radicals in our atmosphere.[1−5] The importance of halogen radical chemistry in the stratosphere is well-appreciated; however, it has been suggested that halogen atoms could also be significant oxidants in the troposphere as Raff et al. have proposed an efficient heterogeneous pathway to $ClNO_x$ that would serve as a source of chlorine atoms.[6] It is known that halogen atom reactions in both gas- and condensed-phase environments will typically involve weakly bound prereactive donor−acceptor complexes (adducts) involving the halogen atom as an acceptor,[3,7,8] and the presence of these complexes can alter both the rate and selectivity of reaction.[7] For example, Breslow and co-workers used a complex between chlorine and pyridine to alter the selectivity of steroid chlorinations.[9] In this case, the selectivity was rationalized in terms of formation of a two-center three-electron bond between the chlorine acceptor and the nitrogen-containing base, and this interaction was subsequently examined theoretically by McKee, Nicolaides, and Radom for a series of saturated and unsaturated amines.[10] The characterization of complexes involving halogen atoms has been the target of extensive and ongoing theoretical efforts.[11−19] In particular, the use of density functional theory (DFT) and the development of long-range corrected functionals for accurate prediction of the structures, spectroscopy, and binding energies of halogen atom adducts have recently been emphasized,[17] and issues with spin contamination when using spin-unrestricted wave functions to describe certain halogen atom complexes have been pointed out.[17,20]

Experimental studies of halogen atom complexes have typically proceeded along two lines, (a) infrared spectroscopy in gas and condensed phases, primarily focused on complexes with diatomic molecules such as the hydrogen halides,[21−24] and (b) electronic (UV−visible) spectroscopy in condensed phases, exploiting the intense charge-transfer (CT) transition of these complexes in the near-UV.[25−29] In an elegant experiment, Wittig and co-workers used bond-specific photodissociation of the HCl dimer to detect signatures of the Cl···HCl adduct.[21] Later, Bondybey and co-workers observed the infrared spectrum of the Br···HBr complex following 193 nm photolysis of $(HBr)_n$ (n = 2, 3) complexes in solid Ne,[22] and Miller and co-workers reported infrared spectroscopy of the X···HF (X = Cl, Br, I) complexes in He nanodroplets.[23] Very recently, Anderson and co-workers have probed the infrared spectrum of the Br···HBr complex in p-H_2 matrixes following irradiation and annealing of co-deposited Br_2/HBr/p-H_2 samples.[24]

In contrast, experimental studies of halogen atom complexes with polyatomic molecules have largely, but not completely, relied on electronic spectroscopy, and such studies date from the early 1960s.[25−29] Over the ensuing years, the role that these complexes play in controlling the reactivity of halogen atoms in solution has been increasingly recognized.[7,8,30−34] For example, Chateauneuf reported a solvent-dependent reaction rate for chlorine atoms in solution that was proportional to the ionization energy of the solvent and suggested the formation of a weakly bound chlorine atom−solvent CT complex that influenced both the rate and selectivity of the chlorine atom reactions.[7] Recently,

Received: June 14, 2011
Revised: July 23, 2011
Published: August 02, 2011

time-resolved resonance Raman and ultrafast transient absorbance studies have followed in real time the formation and decay of Cl atom complexes involved in reactions in solution.[15,34−36] Despite these successes, detailed structural elucidation of these complexes has remained elusive. For example, despite numerous studies over the years,[14,37,38] the structure of the prototypical chlorine atom complex with benzene has remained controversial up to the present day, with recent theoretical studies supporting a preference for η_1 coordination.[14,16,17]

In comparison with Cl atom complexes, less is known regarding complexes involving Br atoms.[39−41] Neta and co-workers used pulsed radiolysis to study the complexes of bromine atoms with various halocarbons and reported spectra of Br atom complexes with DMSO, benzene, and various halons including CH_2Br_2, C_2H_5Br, $CHBr_3$, and CBr_4.[42−44] Subsequent studies from our group[45] and others[46−48] have shown that isohalons are primary photoproducts in many of these systems. For example, recent ultrafast studies of CH_2Br_2 and $CHBr_3$ photolysis in solution show prompt formation of the isospecies, which decay over longer time scales to produce a radical pair, with subsequent formation of a Br···solvent complex.[49−51] In related work, Barbara and co-workers used ultrafast spectroscopy to probe the short-time electron-transfer dynamics in Br atom complexes with benzene and other arenes.[52,53] Initial excitation of the Br···C_6H_6 complex led to electron transfer and the formation of a benzene cation radical and bromide anion. The rate of back electron transfer was found to be much faster than the rate of diffusion, and recovery occurred much faster in neat benzene than in dilute solution, which was attributed to quenching by a 2:1 complex that underwent very rapid charge recombination.[52,53]

Matrix isolation spectroscopy is a technique that is complementary to ultrafast spectroscopy,[54] where a transient species of interest is trapped in an inert matrix at low temperature, leading to a drastic lengthening of the lifetime and affording facile interrogation by conventional frequency domain methodologies. In this article, we use pulsed jet discharge sampling matrix isolation[55] to trap and interrogate the complexes of bromine atoms with simple polyatomic halons. By gently discharging these bromine atom precursors at low current levels (i.e., near threshold), we avoid extensive atomization and fragmentation, and such conditions favor the formation of complexes between liberated bromine atoms and the parent halon. We have measured vibrational (infrared) and electronic spectra of the complexes, and the combination of these methods affords quantitative information on the cross section of the CT transitions. Our experimental results are supported by high-level ab initio and DFT calculations, which shed further light on the structure and binding energy of these complexes. We also report studies of the photochemistry of the complexes following excitation into the intense near-UV CT band.

2. EXPERIMENTAL AND THEORETICAL METHODS

The pulsed jet discharge sampling method has been previously described in detail, as has the apparatus used in this work.[55] Briefly, these experiments utilized a home-built discharge source coupled to a cryostat based on a closed cycle He displex (ARS DS202E). The source was based on a solenoid activated pulsed nozzle that produced gas pulses of 1 ms duration at a variable repetition rate (typically 5−20 Hz). The gas pulse traveled down a short channel before being discharged (−600 V; ∼1.0 mA) between two aluminum ring electrodes, and the discharge products were subsequently deposited on a KBr window held at 23 (Ar) or 7 K (Ne). During deposition, the discharge current and stability were monitored using the voltage drop across a small (100 Ω) resistor placed in the discharge circuit. After deposition, the samples were cooled to the base temperature of the cryostat, ∼5 K. The CH_2BrX (X = H, Cl, Br)/rare gas (∼1:500) samples were generated by passing the high-purity rare gas (Ar, Ne) over the liquid held in a stainless steel bubbler that in turn was placed in a refrigerated, temperature-controlled bath. Before each experiment, the sample line was pumped under vacuum to remove any volatile impurities. Typical deposition conditions were a 5 Hz repetition rate and 1 h deposition time.

Infrared spectra were obtained with a FTIR spectrometer (Mattson, Galaxy series) equipped with a DTGS detector, which was purged at a flow rate of 20 L/min using a purge gas generator (Parker-Balston 75-52A). IR spectra were recorded at 2 cm^{-1} resolution and typically averaged over 128 scans. UV−visible spectra (200−1100 nm) were obtained using an Agilent diode

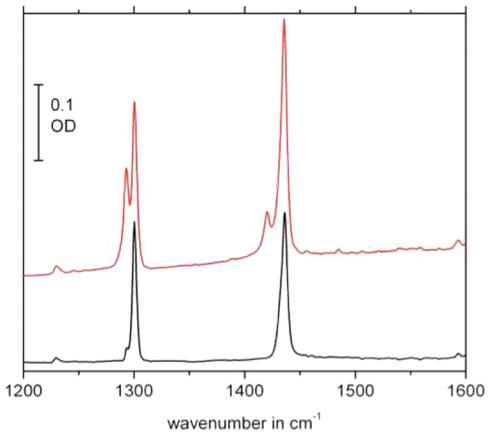

Figure 1. Infrared spectrum of a CH_3Br/Ar (1:220) matrix following pulsed deposition on a KBr window at 23 K and subsequent cooling to 5 K, with (red, upper) and without (black, lower) discharge.

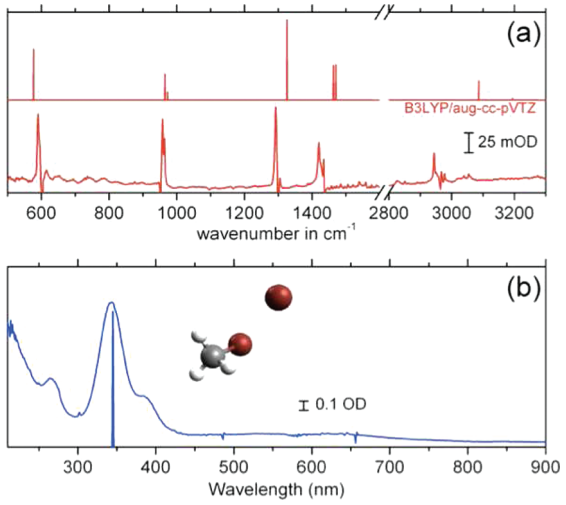

Figure 2. (a) The difference spectrum of the scans shown in Figure 1, compared with the predicted IR spectrum of the Br···$BrCH_3$ complex. (b) The corresponding UV−visible spectrum of the complex, with the predicted spectrum at the TD CAM-B3LYP/aug-cc-pVTZ level.

Table 1. Calculated and Observed Vibrational Frequencies, Intensities of the Br···$BrCH_2X$ (X = H, Cl, Br) Complexes

			calculated (aug-cc-pVTZ basis)			observed
species	mode	approximate description	B3LYP	MP2	M06	Ne (*Ar*)
Br···$BrCH_3$	ν_1	CH_3 torsion	54 (0.0)	85 (0.0)	105 (1.8)	
	ν_2	C−Br−Br bend	77 (2.4)	98 (0.1)	110 (6.6)	
	ν_3	Br−Br stretch	115 (4.0)	107 (19)	144 (0.1)	
	ν_4	C−Br stretch	575 (14)	641 (11)	618 (10)	588 (*590*)
	ν_5	CH_3 rock	965 (7.0)	992 (4.6)	952 (4.8)	952 (*954*)
	ν_6	CH_3 rock	973 (2.2)	996 (2.3)	958 (2.3)	952 (*958*)
	ν_7	CH_3 sym. def.	1326 (22)	1354 (19)	1312 (17)	1284 (*1295*)
	ν_8	CH_3 a. def.	1463 (9.3)	1489 (9.4)	1433 (10)	
	ν_9	CH_3 a. def.	1470 (9.6)	1493 (7.6)	1440 (8.9)	1427 (*1426*)
	ν_{10}	CH_3 a. stretch	3087 (5.2)	3118 (7.5)	3070 (8.2)	2969 (*2962*)
	ν_{11}	CH_3 sym. str.	3194 (0.5)	3240 (0.5)	3188 (0.2)	
	ν_{12}	CH_3 sym. str.	3204 (0.0)	3244 (0.1)	3191 (0.2)	
Br···$BrCH_2Cl$	ν_1	CH_2 torsion	31 (6.3)	44 (5.8)	64 (1.2)	
	ν_2	C−Br−Br bend	45 (1.2)	61 (1.1)	79 (4.9)	
	ν_3	Br−Br stretch	107 (2.9)	92 (12)	103 (4.1)	
	ν_4	C−Br−Cl scis.	218 (0.3)	233 (1.0)	224 (0.2)	
	ν_5	C−Br str.	571 (56)	635 (25)	606 (35)	600 (*599*)
	ν_6	C−Cl str.	726 (110)	784 (106)	753 (119)	752 (*744*)
	ν_7	CH_2 rock	861 (1.9)	881 (2.1)	856 (1.8)	
	ν_8	CH_2 twist	1133 (0.3)	1163 (0.3)	1134 (0.4)	
	ν_9	CH_2 wag	1243 (70)	1263 (63)	1222 (70)	1227 (*1230*)
	ν_{10}	CH_2 scis.	1444 (1.2)	1467 (1.3)	1412 (0.4)	
	ν_{11}	CH_2 sym. str.	3139 (0.6)	3160 (0.5)	3111 (1.2)	
	ν_{12}	CH_2 asym. str.	3227 (4.3)	3249 (4.9)	3192 (1.6)	3054 (*3046*)
Br···$BrCH_2Br$	ν_1	CH_2 torsion	21 (5.1)	40.9 (4.7)	46 (4.3)	
	ν_2	C−Br−Br bend	38 (1.0)	53 (0.9)	70 (3.9)	
	ν_3	Br−Br stretch	102 (2.6)	91 (12)	100 (3.7)	
	ν_4	C−Br−Br scis.	168 (0.3)	180 (1.9)	171 (0.5)	
	ν_5	C−Br asym.	564 (17)	611 (3.2)	592 (5.4)	583 (*582*)
	ν_6	str.	616 (100)	697 (86)	666 (82)	650 (*644*)
	ν_7	C−Br sym. str.	821 (3.2)	843 (3.6)	801 (3.3)	
	ν_8	CH_2 rock	1103 (0.3)	1135 (0.3)	1083 (0.3)	
	ν_9	CH_2 twist	1211 (84)	1232 (77)	1182 (75)	1194 (*1194*)
	ν_{10}	CH_2 scis	1431 (1.9)	1453 (1.8)	1398 (2.1)	
	ν_{11}	CH_3 sym. str.	3143 (0.3)	3165 (0.3)	3109 (0.3)	
	ν_{12}	CH_2 asym. str.	3234 (6.4)	3255 (7.0)	3191 (3.4)	3052

array spectrophotometer, with a typical integration time of 1 s. All spectra were referenced to the cold sample window and subsequently transferred to a spreadsheet and analysis program (Origin 8.0) for workup.

Calculations were carried out on a local (Pere) 128 node cluster using the Gaussian 09 suite of electronic structure programs.[56] All stationary points were characterized by calculating the associated harmonic vibrational frequencies. Geometry optimizations were performed using the B3LYP and M06 density functionals and second-order Moller−Plesset perturbation theory (MP2), with an augmented correlation-consistent triple-ζ quality basis set (aug-cc-pVTZ). Calculations performed on these and related molecules have found that the geometrical parameters are almost converged with respect to a further increase in basis set description (i.e., from a triple-ζ to a quadruple-ζ quality basis set). Electronic absorptions and oscillator strengths were calculated using time-dependent DFT methods, with the B3LYP, CAM-B3LYP, M06, and M06-2X functionals and the same basis set. Our rationale for this choice of methods is described in more detail below. To gain insight into the bonding in these complexes, we carried out calculations on the MP2/aug-cc-pVTZ optimized structures using natural resonance theory (NRT),[57−59] as implemented in the NBO program.[60]

3. RESULTS AND DISCUSSION

A. Spectroscopy and Structure of the Complexes. Figure 1 displays infrared spectra of matrixes obtained by 30 min deposition of a 1:220 CH_3Br/Ar mixture without discharge (red, upper trace) and discharge sampling of the same mixture (black, lower trace). In the discharge sampled spectrum, new features are observed close to the parent CH_3Br absorptions, which can be

assigned to the Br···$BrCH_3$ complex. This complex forms in good yield when deposition occurs at an elevated surface temperature (23 K for Ar). In Figure 2a is shown the difference spectrum of the discharged versus undischarged sample, together with a stick spectrum depicting the calculated spectrum of the complex at the B3LYP/aug-cc-pVTZ level. The full set of vibrational frequencies (in cm^{-1}) calculated at the B3LYP, M06, and MP2 levels with an aug-cc-pVTZ basis set is given in Table 1, along with the experimentally determined frequencies in Ar and Ne matrixes. Note that the calculated $^{79}Br-^{81}Br$ isotope splittings for the vibrations measured here were uniformly small, on the order of a few cm^{-1} or less, and were not resolved in the experiment. In general, there is very good accord between the calculated and observed frequencies (Table 1).

Table S1 (Supporting Information) lists the optimized geometrical parameters of the complex, which shows a Br−Br bond length of ∼3 Å and a strongly bent C−Br−Br linkage (∠C−Br−Br ≈ 90°). This structure is readily understood from a consideration of the charge density surrounding the Br atom in CH_3Br. As discussed by Politzer and co-workers,[61] calculations of the electrostatic potential show a belt of negative electrostatic potential surrounding the halogen atom and a positively charged region centered on the C−Br axis referred to as the σ-hole. This reflects the (small) extent of sp hybridization of the unshared s valence electrons on the Br atom in CH_3Br. In formation of the complex, the electrophilic Br atom is attracted to this negatively charged belt, and thus, the equilibrium geometry features a C−Br−Br angle near 90°. NRT calculations show that only one alpha and one beta spin reference structure, each pictured in Figure S1 in the Supporting Information, make a significant contribution. Analysis of the natural charges shows little CT in the ground state of the complex, with a charge of ∼−0.10 on the terminal Br atom (Table 2). The calculated natural spin density on this bromine atom is 0.89, indicating that most of the radical character still resides on the bromine atom even after complex formation. A fraction of the spin density of ∼0.12 is shared with the bromine atom attached to the halon via the ∼3 Å Br−Br interaction.

Table 2. Natural Bond Orders, Charges, and Natural Spin Densities in Doublet Br···$BrCH_3$[a]

natural bond orders		natural charge and spin densities		
bond	natural bond order (total)	atom	natural charge	natural spin density
C1−Br2	1.0120	C	−0.53537	−0.01134
C1−H3	0.9946	Br	0.05182	0.12695
C1−H4	0.9946	H	0.20018	0.00107
C1−H5	0.9934	H	0.20018	0.00107
Br2−Br6	0.4970	H	0.19474	−0.00096
		Br	−0.11156	0.88320

[a] Bond orders less than 0.05 are not included.

A characteristic feature of the bromine atom−halon complex is a strong CT band in the UV region. This is illustrated in Figure 2b, which displays the observed UV−visible spectrum of the Br···$BrCH_3$ complex obtained under the same conditions. A prominent absorption band is found at 342 nm, in good agreement with TDDFT predictions at the B3LYP, CAM-B3LYP, M06, and M06-2X levels with an aug-cc-pVTZ basis (Table 3). A stick spectrum showing the TDB3LYP/aug-cc-pVTZ prediction is given in Figure 2b. Assuming that the IR and UV−visible spectra sample the same region in the matrix, the integrated IR and UV absorbance can be combined with calculated IR intensities to estimate the oscillator strength of the CT band. Thus, the integrated absorbance of a given IR band was divided by the calculated intensity (in km/mol, Table 1) to derive a column density in the matrix, and an average was taken over the observed transitions. The oscillator strength of a given electronic (UV/Visible) band was then obtained according to the following formula[62]

$$f = \frac{\int A_{UV}(\tilde{\nu})\, d\tilde{\nu}}{N_{IR}} \times (1.87 \times 10^{-7}\ \text{mol/km}) \quad (1)$$

Table 3. Observed (Ne Matrix) and Predicted Electronic Absorptions (in nm) and Oscillator Strengths (*f*) of the Br···$BrCH_2X$ (X = H, Cl, Br) Complexes

species	states	TD-B3LYP/ aug-cc-pVTZ	TD-CAM-B3LYP/ aug-cc-pVTZ	TD-M06 aug-cc-pVTZ	TD-M06-2X/ aug-cc-pVTZ	Observed λ_{max} (osc. Strength)
Br···$BrCH_3$	D_1	1575.0 (0.0001)	1625.8 (0.0001)	1530.6 (0.0001)	1828.2 (0.0001)	342 (0.2)
	D_2	1433.1 (0.0001)	1507.8 (0.0001)	1403.0 (0.0001)	1671.3 (0.0001)	
	D_3	489.3 (0.0001)	406.2 (0.0001)	456.0 (0.0001)	368.6 (0.0001)	
	D_4	344.8 (0.2546)	335.5 (0.2660)	350.2 (0.2345)	348.0 (0.2396)	
	D_5	252.2 (0.0007)	234.3 (0.0009)	252.0 (0.0005)	232.3 (0.0007)	
Br···$BrCH_2Cl$	D_1	1784.6 (0.0001)	1916.7 (0.0001)	1731.6 (0.0001)	2063.3 (0.0001)	333 (0.2)
	D_2	1602.9 (0.0001)	1723.2 (0.0001)	1589.1 (0.0001)	1871.4 (0.0001)	
	D_3	519.0 (0.0001)	416.9 (0.0001)	478.4 (0.0001)	369.6 (0.0001)	
	D_4	392.7 (0.0866)	346.2 (0.2479)	374.7 (0.1597)	343.2 (0.2181)	
	D_5	346.7 (0.1599)	277.8 (0.0055)	338.1 (0.0000)	256.5 (0.0022)	
	D_6	250.1 (0.0048)	262.8 (0.0000)	338.0 (0.0646)	240.5 (0.0000)	
Br···$BrCH_2Br$	D_1	1771.5 (0.0001)	1902.4 (0.0001)	1719.3 (0.0001)	2056.8 (0.0001)	351 (0.2)
	D_2	1597.0 (0.0001)	1717.5 (0.0001)	1590.0 (0.0001)	1857.1 (0.0001)	
	D_3	519.1 (0.0001)	412.0 (0.0001)	474.3 (0.0001)	366.3 (0.0001)	
	D_4	460.1 (0.0481)	356.6 (0.2370)	414.3 (0.0792)	353.1 (0.2172)	
	D_5	445.3 (0.0000)	300.6 (0.0246)	391.1 (0.0001)	280.7 (0.0103)	
	D_6	355.6 (0.2025)	299.6 (0.0000)	353.4 (0.1509)	276.7 (0.0000)	

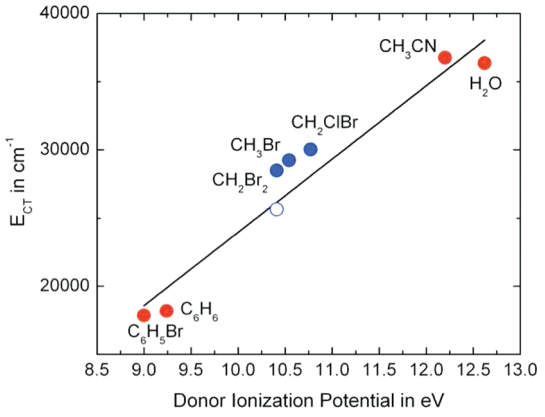

Figure 3. Mulliken plot of the CT band energy (in cm^{-1}) versus the donor ionization energy for a range of Br atom complexes with various donors, as described in the text. For the CH_2BrX complexes, the closed circles represent data from the present study, and the open circle is the value measured for the Br···Br_2CH_2 complex by Shoute and Neta in cyclohexane solution (refs 43 and 44).

where N_{IR} is the column density derived from the IR measurements. Using this approach, the derived oscillator strength of the CT band is 0.2, consistent with the TDDFT predictions (Table 3).

These measurements were extended to bromine atom complexes with other halons, including CH_2Br_2 and CH_2BrCl. The positions of the observed IR absorptions of the Br···$BrCH_2Cl$ and Br···Br_2 CH_2 complexes in Ar and Ne matrixes are compared in Table 1 with calculations performed at the same levels of theory as that above. In both cases, excellent agreement is observed. We note that in the case of CH_2ClBr, because all observed IR absorptions (Table 1) are associated with the CH_2ClBr chromophore, in principle, four different isomers could contribute to the spectrum, Br···$BrCH_2Cl$, Br···$ClCH_2Br$, Cl···$BrCH_2Cl$, and Cl···$ClCH_2Br$. Considering the former two, our calculations of the binding energies, described in detail below, show that the stabilization energy of the Br···$BrCH_2Cl$ complex is around twice that of Br···$ClCH_2Br$, and therefore, Br···$BrCH_2Cl$ is the global minimum-energy structure. Formation of the Cl···$BrCH_2Cl$ and Cl···$ClCH_2Br$ complexes relies on the C−Cl bond being broken in the discharge. In the IR spectrum, transitions due to the CH_2Br and CH_2Cl radical can be identified in the as-deposited matrix, and using the measured IR intensities and calculated (B3LYP/aug-cc-pVTZ) intensities, the ratio of column densities for these two radicals is $N(CH_2Br)/N(CH_2Cl) \approx 1{:}3$. Thus, a minor contribution from the Cl···$BrCH_2Cl$ complex and, to a lesser degree, the Cl···$ClCH_2Br$ complex is expected. In practice, it is difficult to separate this contribution experimentally as the predicted spectra of the two (Br,Cl) complexes are very similar in both the IR and UV. For example, the predicted (B3LYP/aug-cc-pVTZ) IR absorptions of the Cl···$BrCH_2Cl$ and Br···$BrCH_2Cl$ complexes are similar to within 2 cm^{-1}, which would be difficult to detect in our experiment.

The geometrical parameters of the optimized structures of these complexes are given in Table S1 (Supporting Information). The NRT analysis of these complexes yielded very similar results to those found above for the Br···$BrCH_3$ complex, and the details are provided in the Supporting Information. The positions and derived experimental oscillator strengths of the CT band for these complexes are compared with theoretical expectations in Table 3. Again, good agreement is observed. It is important to note that the position of the CT band for the Br···Br_2CH_2 complex observed here (λ_{max} = 351 nm in Ne) is significantly shifted from the position reported by Shoute and Neta in solution (390 nm).[42−44] Previous studies of the UV spectra of Br atom complexes have shown significant solvochromatic shifts, which, interestingly, are much larger than those found for the corresponding molecular halogen complexes. For example, the absorption maximum of the Br···C_6H_6 complex in an Ar matrix (λ_{max} = 469 nm) is significantly blue-shifted from the position observed in solution (λ_{max} = 535−560 nm, solvent-dependent).[26,63−66]

In order to understand the observed solvochromatic shifts, we turn to the formalism developed by Mulliken.[67−69] In this model, the wave function of a donor−acceptor complex D···A is described as a linear combination of zeroth-order wave functions corresponding to a "no-bond" configuration (ψ_0), representing the separated constituents, and a "dative" (ψ_1) configuration corresponding to the $D^{+\bullet}\cdots A^{-\bullet}$ ion pair that follows electron transfer from the donor to acceptor. The solution of the secular determinant gives the transition energy as follows[66,70]

$$E_{CT} = \frac{1}{1-S^2}[(I_D - C)^2 + 4\beta_0\beta_1]^{1/2} \quad (2)$$

where S represents the overlap integral of the no-bond and dative wave functions and I_D is the ionization energy of the donor. The terms β_0 and β_1 represent resonance integrals, which are related according to the expression

$$\beta_1 = \beta_0 - S(I_D - C) \quad (3)$$

In eqs 2 and 3, the term C is related to the electron affinity of the acceptor and also contains electrostatic terms related to the solvation energy of the ions and the ion pair electrostatic interaction. This can be expressed as[70]

$$C = E_A + \frac{e^2}{2}\left(1 - \frac{1}{\varepsilon}\right)\left(\frac{1}{r_{D^+}} + \frac{1}{r_{A^-}}\right) + \frac{e^2}{r_{DA}\varepsilon} \quad (4)$$

where E_A is the electron affinity of the acceptor, ε is the dielectric constant of the medium, and the three radii represent, respectively, the solvent cavities around the donor and acceptor and the donor−acceptor distance in the complex.

In modeling the solvent dependence of the CT excitation energy, we used values for S (=0.1) and β_0 (=−0.94 eV) that were previously determined for Br···arene complexes.[66] The molar volume of the donor was used to calculate the radius of a donor molecule, which was assumed to be the same for the cation radical. This radius added to that of bromine (1.14 Å)[71] provided an estimate for the radius of the complex (r_{DA}), while the radius of the acceptor anion was taken as the ionic radius of the bromide anion (1.96 Å).[71] Using these parameters together with the dielectric constant of solid Ne (ε = 1.24)[72] and Ar (ε = 1.67)[72] gives E_{CT} of 4.07 (Ne) and 3.39 eV (Ar) for the Br···Br_2CH_2 complex, corresponding to excitation maxima of 302 (Ne) and 366 nm (Ar), in reasonable agreement with our experimental values of 351 (Ne) and 356 nm (Ar). When the dielectric constant is changed to that of cyclohexane (ε = 2.0), the predicted position of this band shifts to 400 nm, which is in good agreement with the position reported by Shoute and Neta in cyclohexane solution.[42,44]

Table 4. Predicted Binding Energies (in kcal/mol, including Zero-Point Energy) of the Br···$BrCH_2X$ (X = H, Cl, Br) Complexes

species	B3LYP/aug-cc-pVTZ	MP2/aug-cc-pVTZ	M06/aug-cc-pVTZ	CCSD(T)-aug-cc-pVTZ//M06/aug-cc-pVTZ
Br···$BrCH_3$	6.9	5.9	7.7	5.3
Br···$BrCH_2Cl$	5.9	5.5	7.1	5.3
Br···$BrCH_2Br$	6.0	5.7	7.2	5.3

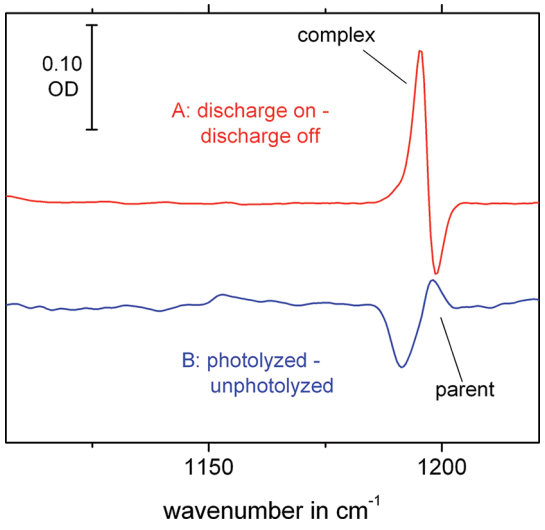

Figure 4. Difference spectra illustrating the formation and destruction of the Br···Br_2CH_2 complex. In the red (upper) trace, the difference spectrum of discharge on and off is shown. The loss of the parent absorption near 1200 cm^{-1} and growth of the complex band at slightly lower cm^{-1} is apparent. Upon photolysis of the complex at 355 nm (blue or lower trace), the complex bands decrease, and the parent band increases.

Equations 2−4 show that for a given acceptor, the energy of the CT band should scale approximately linearly with the ionization energy of the donor, which is the Mulliken correlation. Figure 3 shows a plot of E_{CT} (in eV) versus the donor ionization energy (in eV) for a range of Br atom complexes with various donors, including those studied here and H_2O,[70] CH_3CN,[50] C_6H_6,[73] and C_6H_5Br.[64] Given the sensitivity of the CT band position to environment, a quite reasonable linear correlation is observed among this set of complexes.

B. Binding Energy of the Complexes. The binding energy of the complex was initially calculated using the B3LYP, M06, and UMP2 methods in combination with an aug-cc-pVTZ basis set and corrected for zero-point energy. The predicted values, shown in Table 4, vary from 5.9 (UMP2) to 7.7 kcal/mol (M06) for the Br···$BrCH_3$ complex, and similar results are obtained for the other Br···$BrCH_2X$ complexes examined. As noted above, the calculated binding energy of the Br···$ClCH_2Br$ complex is around 1/2 of this value, that is, between 3 and 3.5 kcal/mol. The use of DFT methods to calculate the binding energy of halogen atom−molecule complexes has been discussed at some length in the literature.[17,74] Croft and Howard-Jones performed a systematic evaluation of DFT and ab initio methods for predicting the binding energy of the prototypical chlorine atom−benzene complex.[17] While many standard DFT methods such as B3LYP lack long-range electron correlation and are therefore suspect for the calculation of binding energies of weakly bound complexes,[75] there are a number of recently developed functionals recommended for noncovalent interactions, including Truhlar's M06 family of functionals.[76] For the complexes examined here, M06 and B3LYP gave similar results for the binding energies, slightly higher than the UMP2 value.

As an additional test, we carried out single-point CCSD(T)/aug-cc-pVTZ calculations on the optimized M06/aug-cc-pVTZ structures, with zero-point corrections taken from the M06/aug-cc-pVTZ calculations. The results of these calculations are also shown in Table 4. Overall, the CCSD(T) results are in very close agreement with the MP2 values and consistently smaller than the B3LYP or M06 predictions. Globally, our calculations predict binding energies near 5 kcal/mol for all of the complexes examined. The effect of basis set superposition error was evaluated using the counterpoise method, and the derived correction was small, < 0.5 kcal/mol.

C. CT Photochemistry of the Complexes. The CT photochemistry of the matrix-isolated complexes was investigated by selective laser wavelength irradiation at 355 nm using the frequency-tripled output of a Minilite-II Nd:YAG laser. In all cases, CT excitation led to the loss of the bands of the complex in the UV and IR and the rise of bands assigned to the uncomplexed parent halon, as illustrated in Figure 4. This can be explained by the following scheme. First, excitation into the CT band leads to rapid CT and formation of a $Br^-\cdots BrCH_2X^{+\bullet}$ ion pair

$$\bullet Br\cdots BrCH_2X + h\nu_{CT} \rightarrow Br^-\cdots BrCH_2X^{+\bullet} \quad (5)$$

In the matrix cage, back electron transfer is expected to be rapid, leading to re-formation of a hot complex that will rapidly dissociate, with subsequent diffusion yielding a separated pair

$$Br^-\cdots BrCH_2X^{+\bullet} \xrightarrow{k_{BET}} [Br\cdots BrCH_2X]^* \rightarrow Br\bullet + BrCH_2X \quad (6)$$

This scheme accounts nicely for our observations, and is consistent with ultrafast studies of the CT photochemistry of complexes between atomic Br and various arenes.[52,53] For example, considering the Br···C_6H_6 complex, it was found that $k_{BET} \gg k_{diffusion}$, and the recovery occurred much faster in neat benzene than in dilute solution, which was attributed to quenching by a 2:1 complex, which was presumed to undergo very rapid charge recombination.[52,53] The measured k_{BET} for the 1:1 Br···C_6H_6 complex in dilute solution was 0.21×10^{10} s^{-1}, corresponding to a lifetime of ~500 ps. Our experiment, of course, probes the steady-state concentration of photoproducts; however, ultrafast experiments on these complexes that probe directly the time scales for electron transfer would be highly desirable.

4. CONCLUSIONS

Pulsed jet discharge matrix isolation spectroscopy and computational methods have been used to characterize prereactive complexes of Br atoms with simple halons, CH_2XBr (X = H, Cl, Br). We have demonstrated a new method for the production

of these complexes, which combines matrix isolation techniques with a pulsed DC discharge nozzle, where a dilute CH_2XBr (X = H, Cl, Br)/rare gas sample was gently discharged and the products were deposited onto a cold KBr window. The resulting $Br\cdots BrCH_2X$ (X = H, Cl, Br) complexes were characterized by infrared and electronic spectroscopy, supported by ab initio and DFT calculations. Our spectra are in excellent agreement with these calculations, which predict gas-phase binding energies for the complexes of ~5−7 kcal/mol. The CT photochemistry of the matrix-isolated complexes was examined. Following excitation into the CT band, the disappearance of the complex absorptions was accompanied by a growth of the parent halon bands. This is explained by rapid back electron transfer leading to a hot complex that subsequently dissociates. Finally, the CT band energies of these complexes were compared with those of Br atom complexes with other donors and with the predictions of Mulliken theory, and a reasonable linear relationship (Mulliken correlation) was found over a broad range of donor ionization energies.

■ ASSOCIATED CONTENT

Supporting Information. Three figures and five tables of computational data on the complexes, including the results of NBO analysis. This material is available free of charge via the Internet at http://pubs.acs.org.

■ AUTHOR INFORMATION

Corresponding Author
*Email: scott.reid@mu.edu..

■ ACKNOWLEDGMENT

Support of the research by the National Science Foundation (NSF CHE-0717960 S.A.R.; CHE-1011959 R.J.M.) and the donors of the Petroleum Research Fund of the American Chemical Society (PRF 48740-ND6) is gratefully acknowledged. Computational resources at the University of Wisconsin—Madison were also supported by the National Science Foundation (CHE-0840494).

■ REFERENCES

(1) Saini, R. D.; Dhanya, S.; Das, T. N. *Bull. Chem. Soc. Jpn.* **2002**, *75*, 1699–1705.
(2) Talukdar, R. K.; Vaghjiani, G. L.; Ravishankara, A. R. *J. Chem. Phys.* **1992**, *96*, 8194–8201.
(3) Bilde, M.; Sehested, J.; Mogelberg, T. E.; Wallington, T. J.; Nielsen, O. J. *J. Phys. Chem.* **1996**, *100*, 7050–7059.
(4) Bilde, M.; Sehested, J.; Nielsen, O. J.; Wallington, T. J. *J. Phys. Chem. A* **1997**, *101*, 5477–5488.
(5) Urbanski, S. P.; Wine, P. H. *J. Phys. Chem. A* **1999**, *103*, 10935–10944.
(6) Raff, J. D.; Njegic, B.; Chang, W. L.; Gordon, M. S.; Dabdub, D.; Gerber, R. B.; Finlayson-Pitts, B. J. *Proc. Natl. Acad. Sci. U.S.A.* **2009**, *106*, 13647–13654.
(7) Chateauneuf, J. E. *J. Org. Chem.* **1999**, *64*, 1054–1055.
(8) Dneprovskii, A. S.; Kuznetsov, D. V.; Eliseenkov, E. V.; Fletcher, B.; Tanko, J. M. *J. Org. Chem.* **1998**, *63*, 8860–8864.
(9) Breslow, R.; Brandl, M.; Hunger, J.; Turro, N.; Cassidy, K.; Krogh-Jespersen, K.; Westbrook, J. D. *J. Am. Chem. Soc.* **1987**, *109*, 7204–7212.
(10) McKee, M. L.; Nicolaides, A.; Radom, L. *J. Am. Chem. Soc.* **1996**, *118*, 10571–10576.
(11) McKee, M. L. *Chem. Phys. Lett.* **1993**, *209*, 195–200.
(12) Dubernet, M.-L.; Hutson, J. M. *J. Phys. Chem.* **1994**, *98*, 5844–5854.
(13) Roeselova, M.; Jacoby, G.; Kaldor, U.; Jungwirth, P. *Chem. Phys. Lett.* **1998**, *293*, 309–316.
(14) Tsao, M.-L.; Hadad, C. M.; Platz, M. S. *J. Am. Chem. Soc.* **2003**, *125*, 8390–8399.
(15) Wang, D.; Phillips, D. L.; Fang, W.-H. *J. Phys. Chem. A* **2003**, *107*, 1551–1556.
(16) Sumiyoshi, T. *Kokagaku* **2004**, *35*, 39–41.
(17) Croft, A. K.; Howard-Jones, H. M. *Phys. Chem. Chem. Phys.* **2007**, *9*, 5649–5655.
(18) Wang, L.; Liu, J.-y.; Li, Z.-s.; Sun, C.-c. *J. Chem. Theory Comput.* **2005**, *1*, 201–207.
(19) Roeselova, M.; Kaldor, U.; Jungwirth, P. *J. Phys. Chem. A* **2000**, *104*, 6523–6531.
(20) Parkinson, C. J.; Mayer, P. M.; Radom, L. *Theor. Chem. Acc.* **1999**, *102*, 92–96.
(21) Kolessov, A.; Liu, K.; Partin, J. W.; Bezel, I.; Underwood, J.; Wittig, C. *Abstr. Pap. Am. Chem. Soc.* **1999**, *217*, U325–U326.
(22) Lorenz, M.; Kraus, D.; Rasanen, M.; Bondybey, V. E. *J. Chem. Phys.* **2000**, *112*, 3803–3811.
(23) Choi, M. Y.; Douberly, G. E.; Falconer, T. M.; Lewis, W. K.; Lindsay, C. M.; Merritt, J. M.; Stiles, P. L.; Miller, R. E. *Int. Rev. Phys. Chem.* **2006**, *25*, 15–75.
(24) Kettwich, S. C.; Pinelo, L. F.; Anderson, D. T. *Phys. Chem. Chem. Phys.* **2008**, *10*, 5564–5573.
(25) Strong, R. L. Preprints Papers International Symposium on Free Radicals, 5th, Uppsala, Sweden, 1961; pp 68/1−68/22.
(26) Strong, R. L. *J. Phys. Chem.* **1962**, *66*, 2423–2426.
(27) Strong, R. L.; Perano, J. *J. Am. Chem. Soc.* **1967**, *89*, 2535–2538.
(28) Buehler, R. E. *Helv. Chim. Acta* **1968**, *51*, 1558–71.
(29) Buehler, R. E.; Ebert, M. *Nature* **1967**, *214*, 1220.
(30) Chateauneuf, J. E. *Book of Abstracts*, 219th ACS National Meeting, San Francisco, CA, March 26−30, 2000; ORGN-462.
(31) Chateauneuf, J. E. *Chem. Commun.* **1998**, 2099–2100.
(32) Chateauneuf, J. E. *J. Am. Chem. Soc.* **1993**, *115*, 1915–1921.
(33) Foergeteg, S.; Berces, T. *J. Photochem. Photobiol., A* **1993**, *73*, 187–195.
(34) Sheps, L.; Crowther, A. C.; Carrier, S. L.; Crim, F. F. *J. Phys. Chem. A* **2006**, *110*, 3087–3092.
(35) Sheps, L.; Crowther, A. C.; Elles, C. G.; Crim, F. F. *J. Phys. Chem. A* **2005**, *109*, 4296–4302.
(36) Wang, D.; Li, Y.-L.; Ho, W. S.; Leung, K. H.; Phillips, D. L. *J. Org. Chem.* **2002**, *67*, 747–752.
(37) Benson, S. W. *J. Am. Chem. Soc.* **1993**, *115*, 6969–6974.
(38) Taylor, C. K.; Skell, P. S. *J. Am. Chem. Soc.* **1983**, *105*, 120–121.
(39) Barra, M.; Smith, K. *J. Org. Chem.* **2000**, *65*, 1892–1894.
(40) Edwards, J.; Hills, D. J.; Shuddhoda, P. M.; Symons, M. C. R. *J. Chem. Soc., Chem. Comm.* **1974**, 556–557.
(41) Sumiyoshi, T.; Fujiyoshi, R.; Katagiri, M.; Sawamura, S. *Radiat. Phys. Chem.* **2007**, *76*, 779–786.
(42) Alfassi, Z. B.; Huie, R. E.; Mittal, J. P.; Neta, P.; Shoute, L. C. T. *J. Phys. Chem.* **1993**, *97*, 9120–9123.
(43) Shoute, L. C. T.; Neta, P. *J. Phys. Chem.* **1990**, *94*, 7181–7184.
(44) Shoute, L. C. T.; Neta, P. *J. Phys. Chem.* **1990**, *94*, 2447–2453.
(45) George, L.; Kalume, A.; Esselman, B. J.; Wagner, J.; McMahon, R. J.; Reid, S. A. *J. Chem. Phys.* To be submitted.
(46) Li, Y. L.; Zhao, C.; Guan, X.; Phillips, D. L. *Res. Chem. Intermed.* **2005**, *31*, 557–565.
(47) Kwok, W. M.; Zhao, C.; Li, Y.-L.; Guan, X.; Wang, D.; Phillips, D. L. *J. Am. Chem. Soc.* **2004**, *126*, 3119–3131.
(48) Zheng, X.; Fang, W. H.; Phillips, D. L. *J. Chem. Phys.* **2000**, *113*, 10934.
(49) Carrier, S. L.; Preston, T. J.; Dutta, M.; Crowther, A. C.; Crim, F. F. *J. Phys. Chem. A* **2010**, *114*, 1548–1555.
(50) Pal, S. K.; Mereshchenko, A. S.; El-Khoury, P. Z.; Tarnovsky, A. N. *Chem. Phys. Lett.* **2011**, *507*, 69–73.

(51) El-Khoury, P. Z.; Pal, S. K.; Mereshchenko, A. S.; Tarnovsky, A. N. *Chem. Phys. Lett.* **2010**, *493*, 61–66.
(52) Schlief, R. E.; Jarzeba, W.; Thakur, K. A. M.; Alfano, J. C.; Johnson, A. E.; Barbara, P. F. *J. Mol. Liq.* **1994**, *60*, 201–220.
(53) Jarzeba, W. *J. Mol. Liq.* **1996**, *68*, 1–11.
(54) El-Khoury, P. Z.; George, L.; Kalume, A.; Ault, B. S.; Tarnovsky, A. N.; Reid, S. A. *J. Chem. Phys.* **2010**, *132*, 124501.
(55) George, L.; Kalume, A.; Reid, S. A. *Chem. Phys. Lett.* **2010**, *484*, 214–218.
(56) Frisch, M. J.; Trucks, G. W.; Schlegel, H. B.; Scuseria, G. E.; Robb, M. A.; Cheeseman, J. R.; Scalmani, G.; Barone, V.; Mennucci, B.; Petersson, G. A.; Nakatsuji, H.; Caricato, M.; Li, X.; Hratchian, H. P.; Izmaylov, A. F.; Bloino, J.; Zheng, G.; Sonnenberg, J. L.; Hada, M.; Ehara, M.; Toyota, K.; Fukuda, R.; Hasegawa, J.; Ishida, M.; Nakajima, T.; Honda, Y.; Kitao, O.; Nakai, H.; Vreven, T.; Montgomery, J. A., Jr.; Peralta, P. E.; Ogliaro, F.; Bearpark, M.; Heyd, J. J.; Brothers, E.; Kudin, K. N.; Staroverov, V. N.; Kobayashi, R.; Normand, J.; Raghavachari, K.; Rendell, A.; Burant, J. C.; Iyengar, S. S.; Tomasi, J.; Cossi, M.; Rega, N.; Millam, N. J.; Klene, M.; Knox, J. E.; Cross, J. B.; Bakken, V.; Adamo, C.; Jaramillo, J.; Gomperts, R.; Stratmann, R. E.; Yazyev, O.; Austin, A. J.; Cammi, R.; Pomelli, C.; Ochterski, J. W.; Martin, R. L.; Morokuma, K.; Zakrzewski, V. G.; Voth, G. A.; Salvador, P.; Dannenberg, J. J.; Dapprich, S.; Daniels, A. D.; Farkas, Ö.; Ortiz, J. V.; Cioslowski, J.; Fox, D. J. *Gaussian 09*, revision A.11.4; Gaussian, Inc.: Pittsburgh, PA, 2001.
(57) Glendening, E. D.; Badenhoop, J. K.; Weinhold, F. *J. Comput. Chem.* **1998**, *19*, 628–646.
(58) Glendening, E. D.; Weinhold, F. *J. Comput. Chem.* **1998**, *19*, 593–609.
(59) Glendening, E. D.; Weinhold, F. *J. Comput. Chem.* **1998**, *19*, 610–627.
(60) Glendening, E. D.; Badenhoop, J. K.; Reed, A. E.; Carpenter, J. E.; Bohmann, J. A.; Morales, C. M.; Weinhold, F. *NBO*, 5.9 ed.; Theoretical Chemistry Institute, University of Wisconsin—Madison: Madison, WI, 2004.
(61) Politzer, P; Lane, P.; Concha, M. C.; Ma, Y.; Murray, J. S. *J. Mol. Model* **2007**, *13*, 305–311.
(62) Kjaergaard, H. G.; Robinson, T. W.; Brooking, K. A. *J. Phys. Chem. A* **2000**, *104*, 11297.
(63) Buhler, R. E. *Helv. Chim. Acta* **1968**, *51*, 1558–1571.
(64) Bossy, J. M.; Buhler, R. E.; Ebert, M. *J. Am. Chem. Soc.* **1970**, *92*, 1099–1101.
(65) Yamamoto, N.; Kajikawa, T.; Sato, H.; Tsubomura, H. *J. Am. Chem. Soc.* **1969**, *91*, 265–267.
(66) Buhler, R. E. *J. Phys. Chem.* **1972**, *76*, 3220–3228.
(67) Mulliken, R. S. *J. Am. Chem. Soc.* **1952**, *74*, 811.
(68) Mulliken, R. S.; Person, W. B. *Molecular Complexes; A Lecture and Reprint Vol.*; Wiley-Interscience: New York, 1969.
(69) Mulliken, R. S.; Person, W. B. *Annu. Rev. Phys. Chem.* **1962**, *13*, 107.
(70) Treinin, A.; Hayon, E. *J. Am. Chem. Soc.* **1975**, *97*, 1716–1721.
(71) *CRC Handbook of Chemistry and Physics*; CRC Press: Boca Raton, FL, 2008; Vol. 88.
(72) Grosso, G.; Martinelli, L.; Pastori Parravicini, G. *Solid State Commun.* **1978**, *25*, 435–438.
(73) McGimpsey, W. G.; Scaiano, J. C. *Can. J. Chem.* **1988**, *66*, 1474.
(74) Prana, B.; Gomperts, R.; Sordo, J. A. *Chem. Phys. Lett.* **2004**, *392*, 236–241.
(75) Kohn, W.; Mier, Y.; Makarov, D. E. *Phys. Rev. Lett.* **1998**, *80*, 4153–4156.
(76) Zhao, Y.; Truhlar, D. G. *Acc. Chem. Res.* **2008**, *41*, 157–167.